

Anomalous and negative reflection of Lamb waves in mode conversionM. Germano,^{*} A. Alippi, A. Bettucci, and G. Mancuso*Dipartimento S.B.A.I., Sapienza Università di Roma, Via A. Scarpa 16, I-00161 Roma, Italy*

(Received 19 September 2011; published 9 January 2012)

Mode conversion is an important feature of wave propagation used in ultrasonic nondestructive testing with Lamb waves. When a wave packet with a given central frequency, and a correspondent central wavenumber, impinges on the free edge of a plate, the reflected wave generally is a weighed combination of all the possible modes compatible with the given frequency. Under particular conditions, only one wave packet is reflected with a distinct central wavenumber compared to the incident one. In such a case, according to Snell's law, the reflection angle is different from the incident one (anomalous reflection). In this article, experimental results are presented on anomalous reflection on a free edge of a thin plate of a Lamb wave packet; moreover, experimental results are reported on a Lamb wave packet that is reflected at an angle lying on the same side, with respect to the normal direction, of the impinging wave (negative reflection). Negative reflection of Lamb waves has been obtained through mode conversion taking place at the free edge of a thin plate of constant thickness: More precisely, a symmetric $S1$ Lamb mode has been converted into the same mode but with phase velocity antiparallel to group velocity, so obtaining the so-called backward-propagating Lamb wave packet.

DOI: [10.1103/PhysRevB.85.012102](https://doi.org/10.1103/PhysRevB.85.012102)

PACS number(s): 43.20.Gp, 43.20.Mv, 46.70.De

I. INTRODUCTION

Since the pioneering work by Vecelago¹ in 1968 on the existence of left-handed electromagnetic waves, a number of different topics have been introduced and developed both in electromagnetism and acoustics relative to new realms in wave propagation phenomena. The search for materials with definite characteristics gave rise to a series of new tailored crystals, differently called metamaterials,^{2,3} photonic crystals,⁴⁻⁶ and phononic crystals,^{7,8} that may create backward propagation, amplification of evanescent waves, negative refraction effect, and, ultimately, superlenses.^{9,10} Negative refraction index, needed for switching the magnetic field counterphase with respect to the electric one, is proper to electromagnetism, but some of its effects are shared by acoustics as well, when resorting to specific properties of dispersion curves, as in the case of regions of negative slopes, since a main feature both for negative refraction (superlenses effect) and negative reflection, is the opposite flow between phase and group velocities, whatever be the method for producing the effect, be either negative refraction index in special materials or mode conversion in guided ultrasonic waves.¹¹

In this Brief Report, a common feature of acoustic plate waves is properly exploited in order to put into evidence the effect of negative reflection arising from the backward propagating mode of a wave. Particularly, the effect of a beam reflection at angles lying on the same side of the impinging beam is put in evidence for mode $S1$ in steel plates in the MHz frequency region. Acoustic plate modes, commonly known as Lamb waves, do have to satisfy stress-free boundary conditions on the limiting surfaces that link the dilatational and shear components of the wave in such a way as to produce dispersive effects for backward propagation, with energy flowing opposite to the wave vector. Recently, mode conversion between forward- and backward-propagating Lamb waves at the interface between two regions of different thickness of an aluminum plate has been used by S. Bramhavar *et al.* for obtaining negative refraction effect and the focusing of the elastic waves.¹² Actually, in our experiment, negative

reflection of elastic waves has been achieved by using a simple homogeneous plate of constant thickness through mode conversion between forward- and backward-propagating Lamb waves occurring at the free edge of the plate itself.

Lamb wave modes are widely used in nondestructive testing techniques. All structures, indeed, in which one dimension at least is small compared to the others, as in the case of plates, shells, wires, rods, pipes, etc., are suitable for being inspected for cracks and defects through the use of multimode Lamb wave analysis.¹³⁻¹⁶ The highly dispersive multimode analysis became essential for optimal defect detection; preliminary study of interactions between modes multireflected at free edges is a necessary condition for modeling interaction with obstacles, defects, inhomogeneities, holes, cracks, delaminations, inclusions, etc. All these abrupt changes of homogeneity and isotropy is a cause for the scattering of the guided waves that, differently from the bulk case, involves all possible modes, real, complex and imaginary, at the specific frequency, depending on the dispersion equation.

In this Brief Report, the reflection of a Lamb mode wave packet is considered, as it is produced at the free edge of an isotropic and homogeneous steel plate. This will be studied in two different cases: first, when mode conversion takes place between modes bearing the same direction both for the group and the phase velocity (incident mode: $S2$, reflected mode: $S0$) and second, with mode conversion between waves whose envelope frequency is centered on two different regions of the dispersion curve of the same mode (incident and reflected mode: $S1$) so that to concurrent directions of the phase velocities there corresponds an opposite direction of the group velocity. While the first case leads to a reflected angle different from the incident one but on the opposite side with respect to the normal direction (anomalous reflection), the same side for the two angles (negative reflection) is found in the second case.

II. EXPERIMENTAL DETAILS

Preliminary characterization of the plate material was performed, and the wave dispersion curves were derived from

numerical integration of the Rayleigh-Lamb equations, once the ratio between longitudinal, V_ℓ , and shear, V_s , velocities of the bulk waves was properly introduced.¹⁷ A steel plate (thickness 1.99 mm, length 400 mm, width 300 mm) was used, for which the longitudinal and shear velocities were experimentally obtained through a pulse echo technique with multiple reflections, where increasing the number of echoes permits us to increase the precision; to check the plate homogeneity, measurements have been performed at several points of the plate surface: longitudinal bulk wave velocity and shear bulk wave velocity is $V_\ell = 5789 \pm 4$ m/s and $V_s = 3188 \pm 3$ m/s, respectively. As rolled steel plates can have considerable texture, elastic isotropy of the plate used in the experiment has been tested by measuring the phase velocity of the $S1$ Lamb mode propagating along various directions: All the values have been found in the range between 8050 m/s and 8220 m/s within the 2% estimated error. The values of the bulk velocities are then inserted into the Rayleigh-Lamb equations and the dispersion relations obtained. Indeed, Lamb modes result from the coupling of longitudinal and shear vertical (SV, with displacement vector normal to the plate surfaces) components and split into two families, the symmetric and the antisymmetric one, where the symmetry is referred to the motion of the material particle with respect to the plane parallel to and equally distant from the plate surfaces: The symmetric modes satisfy the equation

$$\frac{\tan[k_{ts}d/2]}{\tan[k_{tl}d/2]} = -\frac{4\beta^2 k_{tl} k_{ts}}{(k_{ts}^2 - \beta^2)^2} \quad (1)$$

and the antisymmetric modes the equation

$$\frac{\tan[k_{ts}d/2]}{\tan[k_{tl}d/2]} = -\frac{(k_{ts}^2 - \beta^2)^2}{4\beta^2 k_{tl} k_{ts}}, \quad (2)$$

where k_{tl} and k_{ts} are the transversal components of the wavenumber for longitudinal and shear waves, respectively, ω is the angular frequency, and β is the Lamb wave vector satisfying the relations $k_{tl}^2 = (\omega/V_\ell)^2 - \beta^2$ and $k_{ts}^2 = (\omega/V_s)^2 - \beta^2$.

By solving these equations numerically, one obtains the dispersion curves governing the Lamb modes that propagate in an infinite homogeneous and isotropic plate; they have been numerically integrated,¹⁸ and Fig. 1(a) shows the first three solutions for the symmetric modes named $S0$, $S1$, and $S2$; experiments were performed at two different frequencies, $\nu_1 = 2.3$ MHz and $\nu_2 = 1.371$ MHz, indicated by the two horizontal dashed lines; the corresponding wavelengths for the different modes are also shown. It has to be noted that the $S0$ mode has no cutoff frequency and that, for low wavenumber values, the $S1$ mode has a negative group velocity (proportional to the slope of the tangent at the curve) and a positive phase velocity. That means that a wave packet with a wavenumber β centered in this region would have phase and group velocities pointing to opposite directions, giving rise to what is called a backward-propagating wave packet. Figure 1(b) shows an enlargement of the dispersion curve for the $S1$ mode in the frequency range used in the experiment.

Generation of Lamb waves has been obtained by mode conversion of longitudinal waves launched by a piezoelectric transducer onto a lucite wedge with variable angle, placed on the steel plate: A train wave signal at the transducer generates a

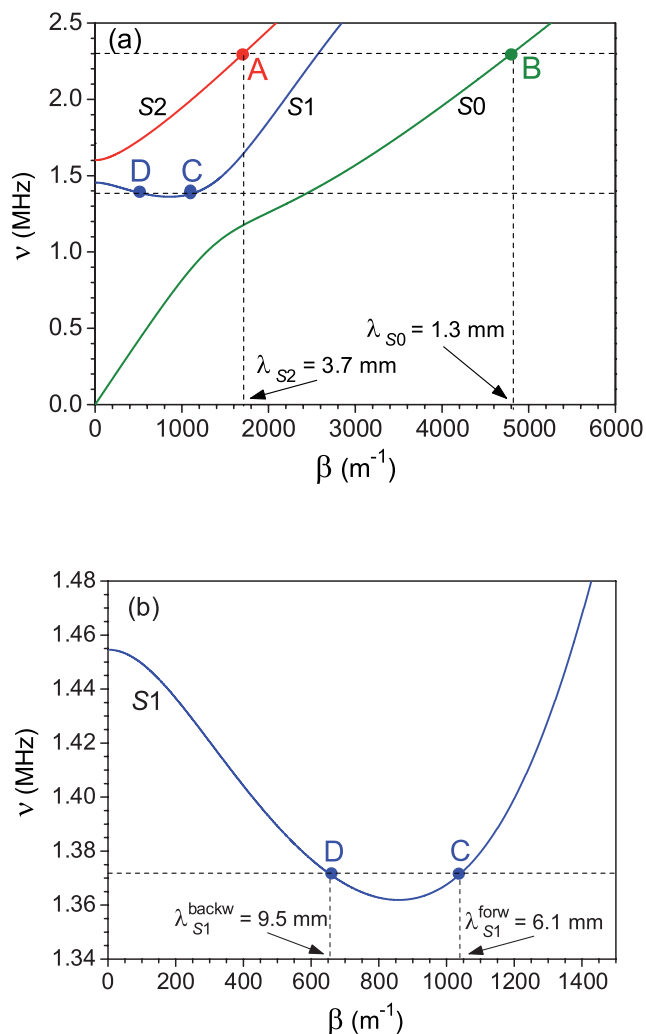


FIG. 1. (Color online) (a) Lamb wave dispersion curves for the first three symmetric modes for the steel plate used in the experiment. (b) Enlargement of the dispersion curve relative to the $S1$ Lamb mode. The horizontal lines are the operating frequencies. The points indicate the central wavenumber of the wave packets: points A and C refer to the $S2$ and the $S1$ incident forward modes, respectively; points B and D are the corresponding converted and reflected $S0$ (forward) and $S1$ (backward) modes. The wavelengths of each mode are also indicated.

longitudinal wave packet, traveling at a speed $V_w = 2720$ m/s in the wedge with wavenumber $k_w = \omega/V_w$, and impinges on the plate surface with an angle ϕ with respect to the normal to the plate surface that selects the Lamb wavenumber β through the relation $\beta = k_w \sin \phi$. The frequency ω and the Lamb wavenumber β ought to match the values on the dispersion curves for the selected mode to be generated.

The Lamb wave packet then impinges on the free edge of the plate at variable angles θ : Stress-free boundary conditions have to be satisfied, and, since the longitudinal component of the Lamb wave changes sign upon reflection while the shearing stress does not, the reflected wave will not only have the same wavelength of the incident wave packet, but it will contain all the possible modes with different wavelengths such as to satisfy the condition of zero traction force at the free

edge. All modes, indeed, may be generated in this process, provided that they have the same symmetry of the incident mode, with real, complex, or imaginary wavenumber, but, for any given frequency, only a finite number of real modes will be reflected as propagating waves.^{19,20} Stress-free conditions are satisfied within an error less than 1% if one considers the first twenty modes at the boundary are considered;²⁰ only a small fraction of them, however, will be reflected as real modes for not too high values of the product frequency times plate thickness. Consequently, experimental conditions can be selected to have an almost complete mode conversion from one impinging mode into just one reflected mode with the same frequency but different wavelength.

III. RESULTS AND DISCUSSION

The reflection by the plate edge of two different Lamb waves has been studied: In the first case, a symmetric $S2$ mode is generated at frequency ν_1 [point A in Fig. 1(a)]; in the second case, a symmetric $S1$ mode is generated at frequency ν_2 [point C in Fig. 1(b)]. For both cases, the driving electric signal sent to the transducer consists of a tone burst 20 cycles long, and, at first, normal incidence on the plate edge has been studied. A laser vibrometer has been used to detect the normal component of the plate surface displacement along a line parallel to the propagation direction of both the incident and reflected wave. Measurements have been carried out along a line where the incident and the reflected wave packet were separated in time so that they have been easily detected and analyzed, leading both to the measure of the phase and group velocity and to the determination of the direction of Poynting vector flow as well.²¹

It has been found that when the $S2$ mode at 2.3 MHz is normally incident on the free edge of the plate, the reflected wave packet is entirely mode converted into the $S0$ mode at the same frequency [point B in Fig. 1(a)], which is consistent with the numerical simulation of mode conversion showing an inessential contribution of $S1$ mode at this frequency-thickness parameter with respect to the other two real modes involved, $S2$ and $S0$.¹⁹ In the second case, when the $S1$ mode at 1.371 MHz is normally impinging on the plate edge, the mode conversion produces a reflected wave packet whose wavenumber is centered around a point lying on the descending branch of the dispersion curve of the $S1$ mode [point D in Fig. 1(b)]: This mode is a backward-propagating wave because the group velocity is antiparallel to the phase velocity.

Once all the involved modes have been identified and their characteristics measured for normal incidence, reflection at oblique incidence to the plate edge has been experimented on. In this case, the spot of the laser vibrometer has been moved along a line parallel to the edge crossing the path of both emitted and reflected beams; at each step, the maximum amplitude of the signal has been measured and a profile of the amplitudes versus direction angle obtained. In Fig. 2, surface vibration amplitude profiles are shown versus the angle of the reflected wave vector directions in the far field approximation in three cases: In (a), the $S2$ Lamb mode impinges at an angle of $\theta_i = +40^\circ$ with respect to the normal and the maximum value of $S0$ reflected mode is centered on

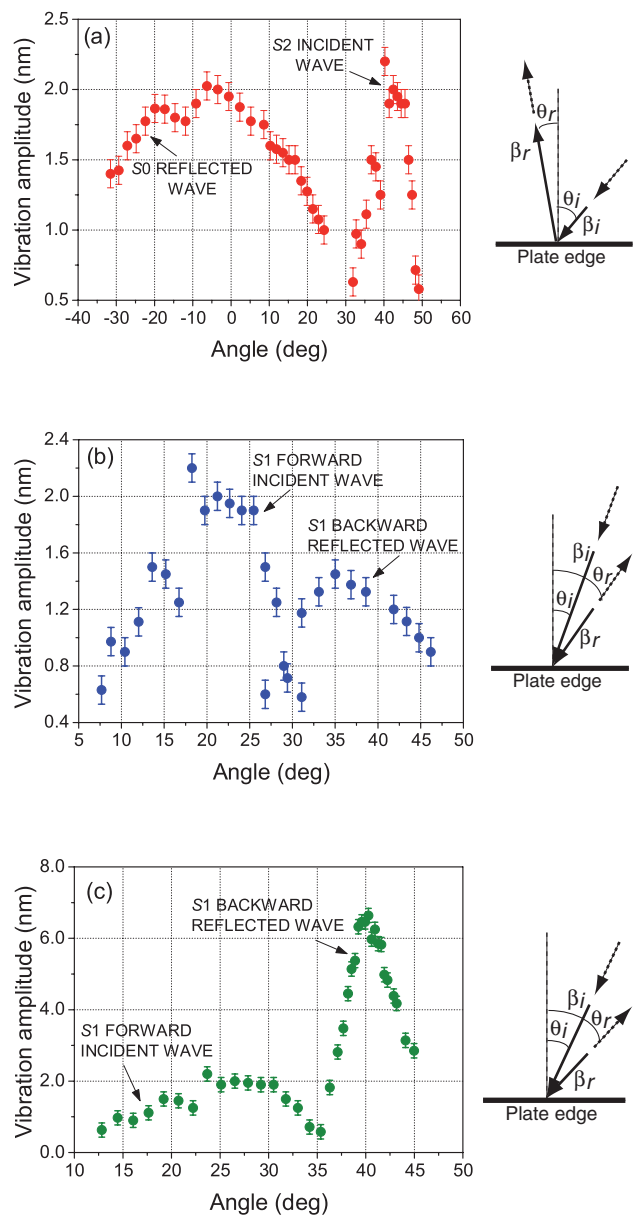


FIG. 2. (Color online) Profiles of the surface vibration amplitudes along a line parallel to the plate edge. On the right side, diagrams of the relative geometrical relationships: the solid vectors refer to wave vectors, the broken ones to energy propagation directions. Case (a): $S2$ forward mode incident on the plate edge at an angle $\theta_i = +40^\circ$ is converted to $S0$ mode and reflected at angle $\theta_r = -13 \pm 2^\circ$ (position of the wave packet center). Mode conversion causes the reflection angle to change from the incident one (anomalous reflection). Case (b): $S1$ forward mode incident on the plate edge at an angle $\theta_i = +20^\circ$ is converted into $S1$ backward mode and reflected at angle $\theta_r = +35 \pm 2^\circ$. Conversion from forward to backward mode causes the angle of reflection to be changed from the incident one and lying on the same side with respect to the normal (negative reflection). Case (c): Same as case (b) but with $\theta_i = +25^\circ$ and $\theta_r = +40 \pm 2^\circ$.

the opposite (negative) side with respect to the normal; the profile of the reflected mode is strongly widened due to the traveled path and the high dispersive properties of the mode. In measurements (b) and (c) of the same figure, the case of the $S1$ incident forward mode (group and phase velocities

having same verse) with $S1$ backward mode (group and phase velocities having opposite verses) reflected is considered for two different values of the incident angle, $\theta_i = +20^\circ$ and $\theta_i = +25^\circ$, (b) and (c) respectively. Amplitude profiles show that the angles of reflection are on the same side, with respect to the normal to the plate surface, of the incident angles. Since the reflected wave is a backward one, the energy (group velocity) is reflected back away from the plate edge while the wavenumber vector (phase velocity) still points toward the plate edge, therefore negative reflection through mode conversion takes place because there is no inversion of the normal component of the incident wavenumber vector.

Snell's law conservation of the tangential wavenumber components is verified as shown by the experimental results: If, following the dispersion curves (see Fig. 1), values of central wavenumber for all the involved modes are assigned, Snell's law provides the angles of reflection in the three cases. In particular, for the first case with $S2$ mode incident at $\theta_i = +40^\circ$ and the $S0$ mode reflected, the corresponding wavelengths are $\lambda_{S2} = 3.7$ mm and $\lambda_{S0} = 1.3$ mm such that the expected angle of reflection of the $S0$ mode is $\theta_r = -\arcsin[\lambda_{S0}/\lambda_{S2} \cdot \sin(40^\circ)] = -13.2^\circ$. For $S1$ forward mode, at a frequency of 1.371 MHz, the wavelength is $\lambda_{S1}^{\text{forw}} = 6.1$ mm, while for the $S1$ backward mode the wavelength is $\lambda_{S1}^{\text{backw}} = 9.5$ mm. When the two incident angles for the $S1$ forward mode are $\theta_i = +20^\circ$ and $\theta_i = +25^\circ$, the expected angles of reflection

for the $S1$ backward mode are $\theta_r = +32.4^\circ$ and $\theta_r = +41.4^\circ$, respectively. Interpolation and fitting of the slightly deformed wave packets received after reflection (see Fig. 2), give for the maxima of the packets the following experimental values for the angle of reflection θ_r : $-13 \pm 2^\circ$ [case (a)], $+35 \pm 2^\circ$ [case (b)], and $+40 \pm 2^\circ$ [case (c)], in good agreement with the theoretical expected values -13.2° [case (a)], $+32.4^\circ$ [case (b)], and $+41.4^\circ$ [case (c)].

IV. CONCLUSIONS

In conclusion, negative or anomalous reflection and negative refraction, as well their applications (ideal perfect lens or focusing plane mirrors), rely on the different or even counterdirected directions for the phase and the group velocities. Such an effect can be obtained through the use of special metamaterials with negative refraction index or, as presented in this Brief Report, through mode conversion phenomena in the field of ultrasonic guided waves. We have shown that Lamb waves mode conversion, at the free edge of a plate of constant thickness, may cause the reflection angle either to change from the incident one (anomalous reflection) or to change from the incident one and lying on the same side, with respect to the normal direction, of the impinging wave (negative reflection). For this latter case, a backward propagating wave, characteristics for Lamb waves have been used.

*massimo.germano@uniroma1.it

¹V. G. Veselago, *Sov. Phys. Usp.* **10**, 509 (1968).

²*Metamaterials: Theory, Design, and Applications*, edited by T. J. Cui, D. R. Smith, and R. Liu (Springer, New York, 2010).

³J. Valentine, S. Zhang, T. Zentgraf, E. Ulin-Avila, D. A. Genov, G. Bartal, and X. Zhang, *Nature (London)* **455**, 376 (2008).

⁴S. John, *Phys. Rev. Lett.* **58**, 2486 (1987).

⁵J. D. Joannopoulos, R. D. Meade, and J. N. Winn, *Photonic Crystals* (Princeton University Press, Princeton, 2008).

⁶E. Cubukcu, K. Aydin, E. Ozbay, S. Foteinopoulou, and C. M. Soukoulis, *Nature (London)* **423**, 604 (2003).

⁷E. N. Economou and M. M. Sigalas, *Phys. Rev. B* **48**, 13434 (1993); *J. Acoust. Soc. Am.* **95**, 1734 (1994).

⁸Z. Liu, X. Zhang, Y. Mao, Y. Y. Zhu, Z. Yang, C. T. Chan, and P. Sheng, *Science* **289**, 1734 (2000).

⁹J. B. Pendry, *Phys. Rev. Lett.* **85**, 3966 (2000).

¹⁰S. Zhang, L. Yin, and N. Fang, *Phys. Rev. Lett.* **102**, 194301 (2009)

¹¹M. Germano, A. Alippi, A. Bettucci, and A. D'Orazio, *J. Acoust. Soc. Am.* **123**, 3834 (2008).

¹²S. Bramhavar, C. Prada, A. A. Maznev, A. G. Every, T. B. Norris, and T. W. Murray, *Phys. Rev. B* **83**, 014106 (2011).

¹³S. Yang, J. H. Page, Z. Liu, M. L. Cowan, C. T. Chan, and P. Sheng, *Phys. Rev. Lett.* **93**, 024301 (2004).

¹⁴A. Sukhovich, L. Jing, and J. H. Page, *Phys. Rev. B* **77**, 014301 (2008).

¹⁵K. F. Graff, *Wave Motion in Elastic Solids* (Dover Publications, Inc., New York, 1975).

¹⁶D. Royer and E. Dieulesaint, *Elastic Waves in Solids* (Springer, Berlin, 2000).

¹⁷B. A. Auld, *Acoustic Fields and Waves in Solids*, 2nd Ed. (R. E. Krieger, Malabar, FL, 1990).

¹⁸E. L. Adler, J. K. Slaboszewicz, G. W. Farnell, and C. K. Jen, *Trans. Ultrason. Ferroelectr. Freq. Control* **37**, 215 (1990).

¹⁹P. J. Torvik, *J. Acoust. Soc. Am.* **41**, 346 (1967).

²⁰B. Morvan, N. Wilkie-Chancellier, H. Dufflo, A. Tinel, and J. Duclos, *J. Acoust. Soc. Am.* **113**, 1417 (2003).

²¹M. Germano, A. Alippi, A. Bettucci, A. Biagioni, D. Conclusio, and D. Passeri, in *Proceedings of Forum Acusticum 2011*, Aalborg (Denmark), June 2011, European Acoustic Association (2011).